CHARACTERIZATION OF BRICK MASONRY: STUDY TOWARDS RETROFITTING URM WALLS WITH TIMBER-PANELS

Jamiu A. Dauda[1], Ornella Iuorio[2], and Paulo B. Lourenço[3]

[1] University of Leeds, School of Civil Engineering, UK
cnjad@leeds.ac.uk

[2] University of Leeds, School of Civil Engineering, UK
o.iuorio@leeds.ac.uk

[3] University of Minho, Department of Civil Engineering, Portugal
pbl@civil.uminho.pt

Keywords: Brick masonry, Characterization, Finite element analysis, Retrofit, Timber-panel, Unreinforced masonry wall.

Abstract. *The overall purpose of this study is to explore the possibility of using timber-panels to retrofit URM walls. However, this paper only present the overall proposed experimental program together with the experimental characterization of mechanical properties of masonry components: units and mortar. The present work developed finite element numerical model that is able to predict the strength of the masonry cube, on the safe side. The numerical model was validated with an experimental test on masonry cube showing 9% difference in the maximum compressive strength of masonry. The modelling technique adopted is the detailed micro modelling where the unit and mortar were represented by their respective mechanical properties using ABAQUS. Because, the numerical results compliment what was observed during the experimental test, then the developed model can be used to predict the general behaviour of masonry wall in the subsequent study.*

Notations

ε_c	:	*Compressive strain*
ε_{c1}	:	*Compressive strain at the peak stress*
ε_{cr}	:	*Tensile strain at cracking*
ε_t	:	*Tensile strain*
σ_c	:	*Compressive stress*
σ_t	:	*Tensile stress*
E_b	:	*Secant modulus of elasticity of masonry unit*
E_{cm}	:	*Secant modulus of elasticity of mortar*
E_{ib}	:	*Tangent modulus of elasticity of masonry unit @ 30% f_b*
f_b	:	*Compressive strength of masonry unit*
f_{cm}	:	*Compressive strength of mortar*
f_{ctm}	:	*Tensile strength of mortar*
f_{tb}	:	*Tensile strength of masonry unit*

1   INTRODUCTION

Prior to the emergence of modern building materials such as concrete and steel, masonry was the predominant oldest building material. Masonry is a configuration of units bonded together with mortar often categorized as homogenous brittle material. Masonry materials are relatively available at low cost and can be easily built with available semi-skilled workers. These make masonry construction to be popular as one of the earliest building typologies. Consequently, substantial amount of unreinforced masonry (URM) structures were built all over the world in the past and now they constitute a unique historical value for civilization. These old URM structures have been found to perform weaker than recent structures when subjected to excessive out-of-plane loading. Because, they were designed and built to construction techniques with no conformity to any construction codes but rather to building's rules of art [1-3]. Therefore, retrofit of old URM is highly encouraged to avert substantial damages and loss of lives when they are subjected to excessive out-of-plane loading.

Existing URM have often little strength to withstand out-of-plane loads. Under severe out-of-plane loading, their failure is likely to be sudden and severe, producing devastating damages, injuries and/or death [4-6]. Out-of-plane loading can be due to an overpressure from blast effect induced by an explosion or earthquake, impacts from snow-avalanche, extreme wind, and more generally wall subjected to normal pressure on the out-of-plane [7].

However, the focus of this study is to examine the behavior of URM walls subjected to out-of-plane loading using quasi-static loading scheme. The reasons for selecting quasi-static loading scheme is that the test will be able to replicate the behavior of URM wall when subjected to cycles of loadings through hydraulic actuator which is similar to what is expected from dynamic effect. Quasi-static loading has been widely accepted and implemented in previous studies in the absence of expensive shaking table or impact loading facilities. This research is not only applicable to earthquakes but to generate knowledge and understanding on whether timber panels can improve the out-of-plane capacity of URM walls against excessive out-of-plane loading in general. Indeed, while timber-panels are currently being used for energy retrofit of old URM buildings; their application in structural retrofitting of URM has still not been fully studied.

An experimental study performed by [8] was among the first study to analyses the application of timber panels as strengthening system for existing buildings against seismic force. [8] studied the in-plane behavior of URM retrofitted with Cross Laminated Timber (CLT) panels and they found that there is considerable increase in strength and ductility of URM. [8] reported a 100% increase in ductility when the CLT panel is connected to URM walls with a specially developed steel connection at top and bottom of the wall. However, the availability of these special connections remains major concerns.

Therefore, this study proposes numerical and experimental investigation on the use of oriented strand board (OSB) and CLT panels for the retrofit of URM walls. The proposed connection typologies are threaded dry rod connections and injectable chemical adhesive readily available in the market.

In this paper, the overall experimental program for the proposed study is presented in section 2, the experimental characterization of mechanical properties of masonry components (UK fired clay solid bricks and mortar) and the compressive strength of masonry cubes is presented in section 3. In section 4, the numerical analysis by finite element developed in ABAQUS to predict the behavior of masonry cubes is presented, and it is based on the detailed micro-modelling techniques described in [9].
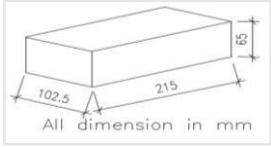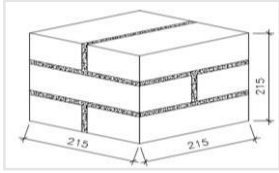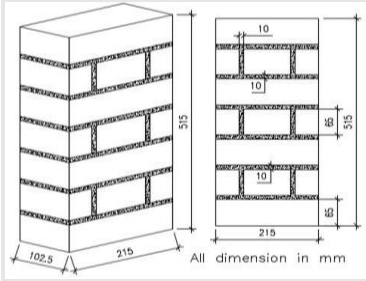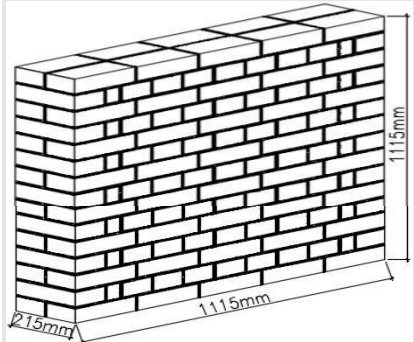
2   EXPERIMENTAL PROGRAM

The proposed experimental campaign is articulated in to three main stages: (a) material characterization, (b) small-scale test: flexural bond strength of masonry prism and (c) full-scale test: out-of-plane flexural strength of masonry wall. Firstly, experimental studies have been carried out to define consistency and compressive strength of mortar and the dry density, water absorption, compressive strength, modulus of elasticity, and Poisson ratio of brick units, all according to the relevant BS and Eurocodes. Compressive strength of masonry composite (215 x 215 x 215mm masonry cube) was also determined.

After that, small-scale experiments will be conducted on fifteen samples of masonry prisms (215 x 515 x 102.5mm) constructed from 215 x 102.5 x 65mm UK standard size engineering class B solid brick and 10mm nominally thick mortar joint (1:1:6, cement:lime:sand). This test will be carried out according to guidance of [10, 11]. The purpose of this test is to provide a simplified means of gathering data on the flexural strength of plain URM prisms and URM prisms retrofitted with two different type of timber panels and two types of connection (Table1). This will help to understand the behavior of masonry wall and the connection between masonry wall and timber panel.

The knowledge gained from the small-scale test will then be used to perform full-scale tests to determine out-of-plane flexural strength of masonry walls. Nine specimens of masonry wall (1115 x 1115x 215mm) will be constructed. This test follows the same principle of the small-scale test according to [10, 11]. The purpose of this test is to evaluate how the timber panel has aided the out-of-plane behavior of the masonry wall. The test walls will be retrofitted using CLT panel and connection type that offer most improvement in the flexural bond strength of masonry prism to be identified from the small-scale test.

Maximum load and out-of-plane displacements values will be recorded at failure states for each of these tests. The results for plain and retrofitted walls will be analyzed and compared to evaluate how timber-panel has aided the out-of-plane behavior of the URM walls. Numerical analysis using commercial Finite Element (FE) software ABAQUS will be performed and validated against the experimental data. The experimental campaign is summarized as shown in table 1 and these will be carried out at George Earle laboratory, school of civil engineering, university of Leeds.

Test Category	Label	γ_{du}	W_u	f_b	E_b	μ_b
Characterization	BR1	Y	Y	Y	N	N
	BR2	Y	Y	Y	N	N
	BR3	Y	Y	Y	N	N
	BR4	Y	Y	Y	Y	Y
	BR5	Y	Y	Y	Y	Y
	BR6	Y	Y	Y	Y	Y
	MC1					
	MC2					
	MC3	Only the compressive strength of MC was de-				
	MC4	termined				
	MC5					
	MC6					

Small scale: masonry prism	Label	TP-T(mm)	Connection	No of test
	PMP	-	-	3
	MPOSBC1	25	C1	3
	MPOSBC2	25	C2	3
	MPCLTC1	60	C1	3
	MPCLTC2	60	C2	3
Full scale: masonry wall				
	PMW	-	-	3
	MWR1S	TP*	C*	3
	MWR2S	TP*	C*	3

$\gamma_{du}, W_u, f_b, E_b, \mu_b$ are dry density, water absorption, compressive strength, modulus of elasticity and poison ratio of brick unit respectively

BR is brick unit

MC is masonry cube

Y means brick units tested for the property

N means brick units not tested for the property

C1 is connection type 1 (mechanical connection)

C2 is connection type 2 (chemical connection)

C* is the best performed connection type in small-scale test

TP-T is the timber panel thickness

TP* is the best performed timber panel in small-scale test

PMP means plain masonry prisms

MPCLTC1 means masonry prism retrofitted with CLT panel using connection type 1

PMW means plain masonry wall

MWR1S means wall retrofitted on one side using CLT

Table 1: Experimental test matrix with indication of specimen's labels

3   EXPERIMENTAL CHARACTERIZATION OF MASONRY COMPONENTS

Prior to designing any retrofit schemes, an understanding of the structural response of the structures is essential. In the case of masonry, its behavior under loading is affected by the mechanical properties of the masonry unit and mortar. These properties were determined experimentally as a prerequisite for investigation of the proposed retrofit techniques.

3.1   Characterization of brick unit

Six samples of engineering class B fired clay solid brick (UK standard size 215 x 102.5 x 65mm) were selected randomly and tested. The bricks were tested in dry condition. The dry density (γ_{du}) of the bricks was determined according to [12] to indicate the general quality and conformity of the brick to manufacturer specification. The bricks were conditioned to constant mass by drying in an oven at $100^{o}C$ temperature for 48hrs, the dry weight and dimensions of the bricks were then obtained using weighing balance and measuring ruler respectively. The γ_{du} was calculated based on weight and volume of bricks. Thereafter, the water absorption (w_u) was determined according [13] to determine the durability of the bricks. The bricks were immersed in cold water for 24hrs and the weight of the saturated bricks were obtained within 2mins after removal from the water. The increase in mass of the brick gives the % w_u of bricks.

The compressive strength (f_b) of the six bricks was also determined according to [14]. This is very important because the compressive strength of masonry depends on the compressive strength of the brick unit and is essential for design and retrofit of masonry. The specimens, after conditioned back to a constant mass, were laid and centered on the platen of a 5000KN capacity compression testing machine with 2mm thick plywood placed top and bottom face of the brick. A uniformly distributed load was then applied gradually in equal increments of 4kN/secs up to failure. The loading and the results were monitored using data logger connected to the machine and f_b was calculated from the failure load and loaded area of the brick. 3 bricks each was loaded on header and bed face respectively (Fig. 1a).

The modulus of elasticity(E_b) was determined using the stress-strain relationship obtained from the axial compression test. Before, placing the bricks under compression machine, FLA-5-11 strain gauges were fixed in longitudinal and along lateral direction on each brick (Fig. 1a) to record the strain values under axial compression. E_b was calculated by considering values between 30% and 60% of maximum stress as done by some other researchers [15, 16]. Also, Poisson ratio (μ_b) was calculated by plotting the lateral strains against longitudinal strains of each bricks. Best line of fit was then plotted to determine the relation between the lateral and longitudinal strain. E_b and μ_b were only determined for bricks loaded in bed face because, the walls under test will be constructed with brick laid in bed face.

3.2   Characterization of mortar

Type N (general purpose) mortar mix with ratio of 1:1:6 (cement: lime: sand) was prepared. The amount of water to be added to mix proportion was not mentioned in standard codes, hence the optimum water content which gives a working consistency was found by trial and error using the dropping ball test described in [17]. The target dropping value of 10 +/- 0.5mm was achieved after three trials. Thereafter, the consistency of the fresh mortar was determined by flow test according to [18].

Three samples of 100 x 100 x 100mm cube were prepared and cured for 28days and tested under compression testing machine to determine the compressive strength of the mortar (f_m). The specimens were carefully aligned under the machine with the center of the ball-

seated platen, so that a uniform seating is obtained, and a uniformly distributed load was applied gradually in equal increments continuously at 1kN/secs up to failure. f_m was calculated from the failure load and loaded area of mortar.
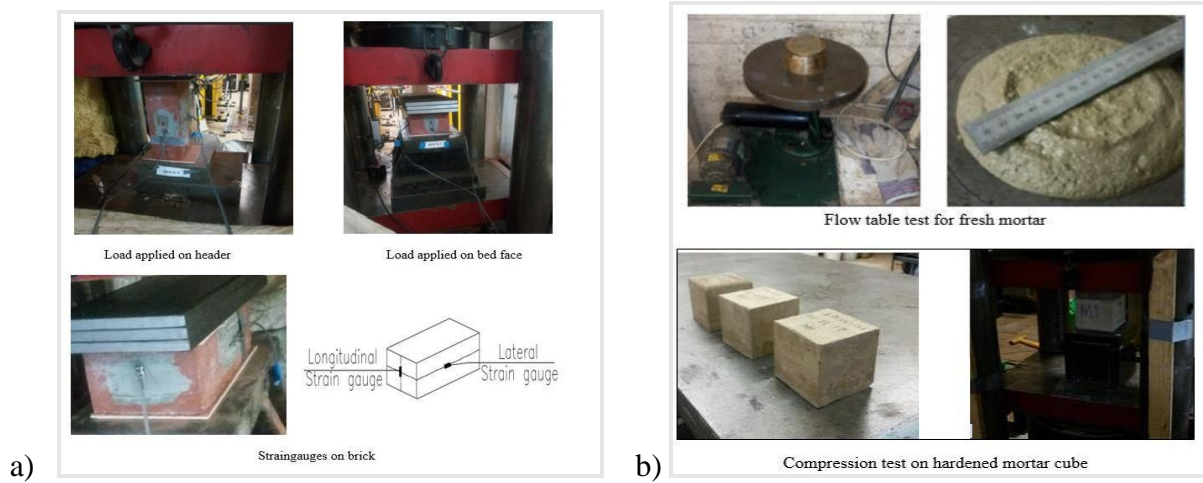

Figure 1: (a) Characterization of masonry unit and (b) Characterization of mortar.

3.3   Characterization of masonry cube

The purpose of this test is to understand how bricks and mortar work together. It is an unconventional test and not to any standard but found in [19]. Six masonry cubes (MC) of 215 x 215 x 215mm were prepared using masonry units from the same stock as ones tested earlier and 10mm thick mortar joint described above. The MC were prepared in the laboratory and horizontal level surface is ensured by using a bubble level during construction. After the construction, each sample was wrapped with polythene sheet for 14days and thereafter open and cured further for 14days in the laboratory to allow the samples to achieve its maximum strength. An attempt to measure the deformation of the MC was made by attaching four LVDTs to the MC before testing (Fig. 2). The specimens were carefully aligned with the centre of the ball-seated platen, under compression testing machine with 2mm thick plywood placed top and bottom under compression testing machine. A uniformly distributed load was applied gradually in equal increments continuously at 4kN/secs rate up to failure.
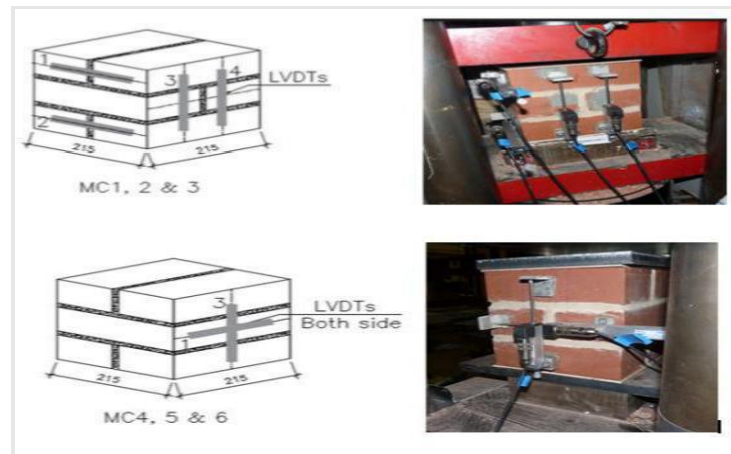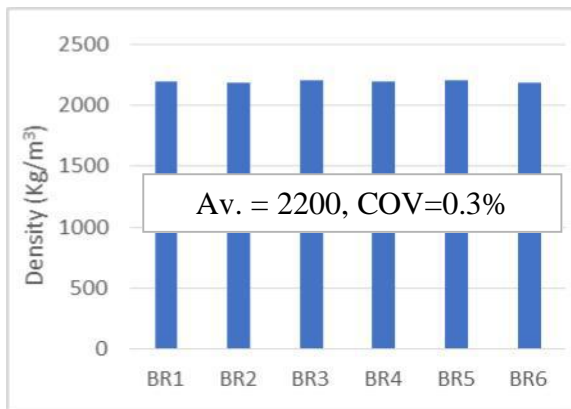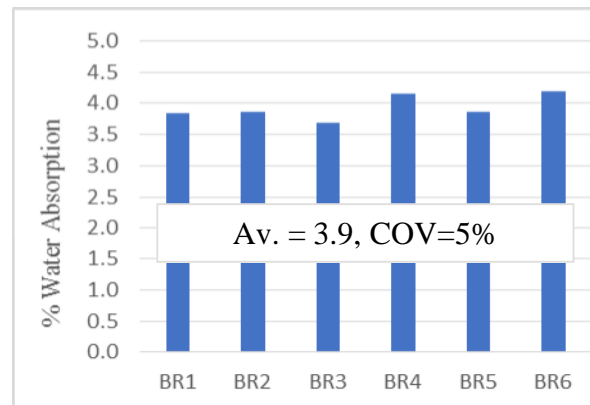

Figure 2: Characterization of masonry cube
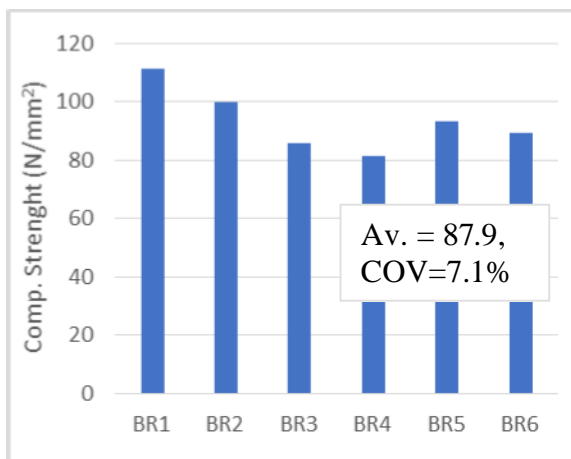
3.4 Experimental results and analysis
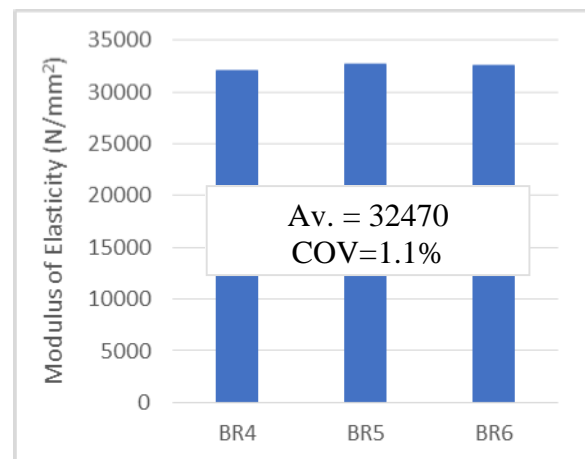
3.4.1 Brick unit
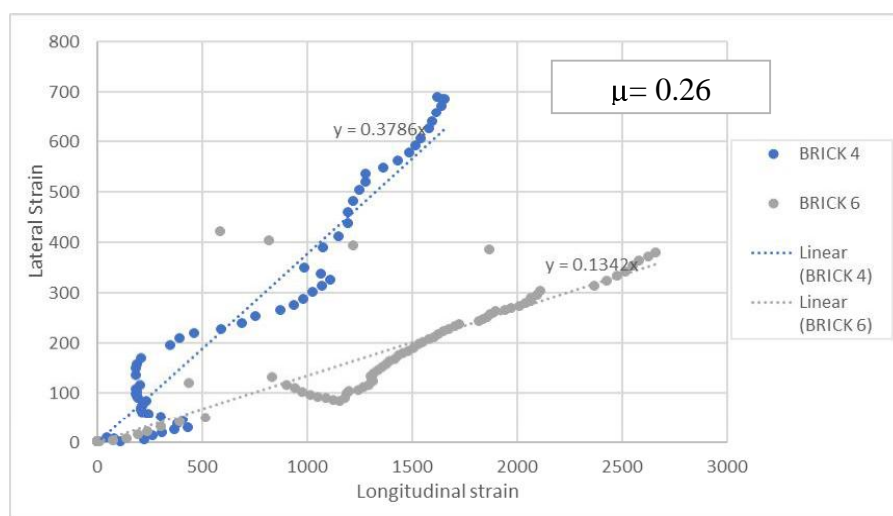

a) Density of brick (kg/m^3)

b) % water absorption rate of brick

c) Compressive strength of brick (N/mm^2)

d) Modulus of elasticity of brick (N/mm^2)

e) Poisson ratio of brick

Figure 3: Mechanical properties of masonry brick.

The obtained brick properties were compared to the values declared by manufacturer except for E_b and μ_b that were compared with values in literatures (Table 2). The strains plot for BR5 is too scatter and the line of fit does not seem best, hence the results was discarded and μ_b calculated using results for BR4 and BR6. Generally, the results indicate that bricks are of good quality and conform to specification, making it acceptable for the proposed experiment.

Property	Values		Requirement
	Experiment	Manufacturer	
γ_{du} (kg/m³)	2200	2310	shall not be less than 2079kg/m³ i.e 90% of specified density [12]
W_u (%)	3.9	≤ 7	shall not be more than manufacturer limit [13]
f_b (N/mm²)	87.9	75	shall be not less than the declared compressive strength[14]
E_b (N/mm²)	32470	≤ 34000	between 3500 and 34000 found in literatures
μ_b	0.26	0.3-0.5	range for clay masonry unit

Table 2: Mechanical properties of masonry brick units.

3.4.2 Mortar

For the fresh mortar, the mix ratio of 1:1:6 with w/c ratio of 0.96 gives the dropping value of 10.2mm and the corresponding mean flow value is 167mm. The consistency of mortar is good as this agreed with the ideal flow value (150-175mm) for embedding masonry as derived from [20]. However, the hardened mortars have an average strength (f_m) of 7.1N/mm²
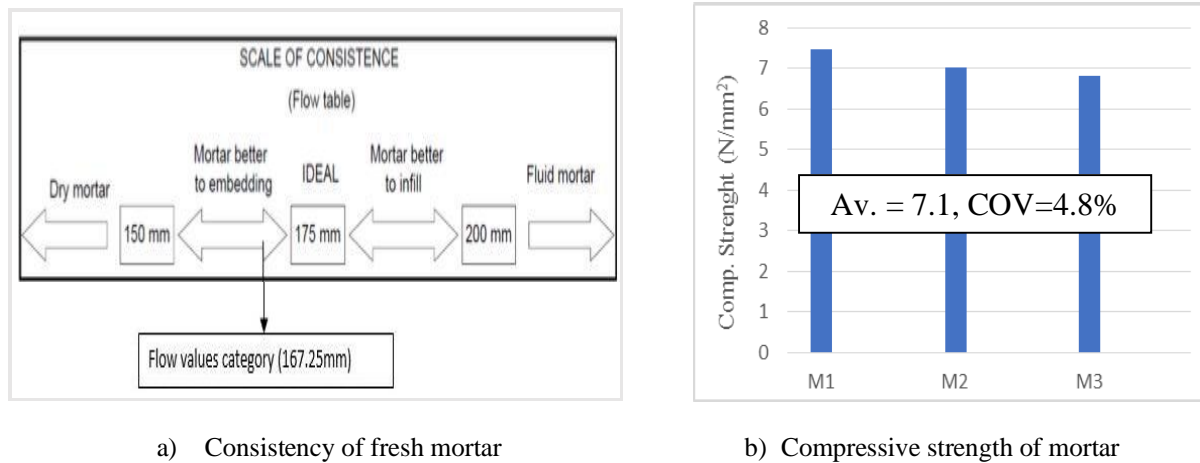

a) Consistency of fresh mortar   b) Compressive strength of mortar

Figure 4: Properties of mortar.

3.4.3 Masonry cube

The average compressive strength of the masonry cube obtained from experiments is 46.4N/mm². Considering the provision of section 10.2 of [21], the compressive strength if found to be 41.4N/mm². Meanwhile [22] described that compressive strength of masonry can be calculated using the properties of the units and mortar according to equation 1. The calculated value 22.5N/mm² is 45% lower than what was gotten experimentally. This seems acceptable because the calculated value is characteristic and a lower bound of many tests.

$$f_k = K \times f_b^{\alpha} \times f_m^{\beta} \qquad (1)$$

Where; f_k : is characteristic compressive strength of masonry

f_b : is compressive strength of masonry unit, in the direction of the applied action

f_m: is compressive strength of the mortar

K: is a constant, which is a function of the type of masonry units and mortar (0.55)

α and β : are constants, for general purpose mortar =0.7 and =0.3

Summarily, the strength obtained for the bricks and mortar shows that the brick is a strong unit while the mortar is a weaker joint which make the combination a strong unit-weak mortar joint connection which is a typical characteristic of old masonry structures.

3.5 Failure mode

Monitoring the failure pattern of both the units and masonry cubes during the test was very difficult because the test rig was enclosed to avoid injuries. The observation of the images after the test shows that the failure modes are brittle. However, an obscure view through the casement and video recorded during tests indicate that the failure of the units starts with a vertical crack along the height of the bricks causing a high tensile stress in the bricks which make them to fails ultimately. For masonry cubes, the failure was characterized by vertical splitting cracks appearing firstly in the central unit and extended to other units as the stress increases. This observation is similar to what was reported by several other authors. This failure pattern is due to lateral expansion of the mortar inducing high tensile strength in the bricks. As can be seen from figure 5, the MC split on the faces caused the attached LVDTS on the surface to fall off which make recording the deformation difficult because the compression machine does not have an inbuilt LVDT.
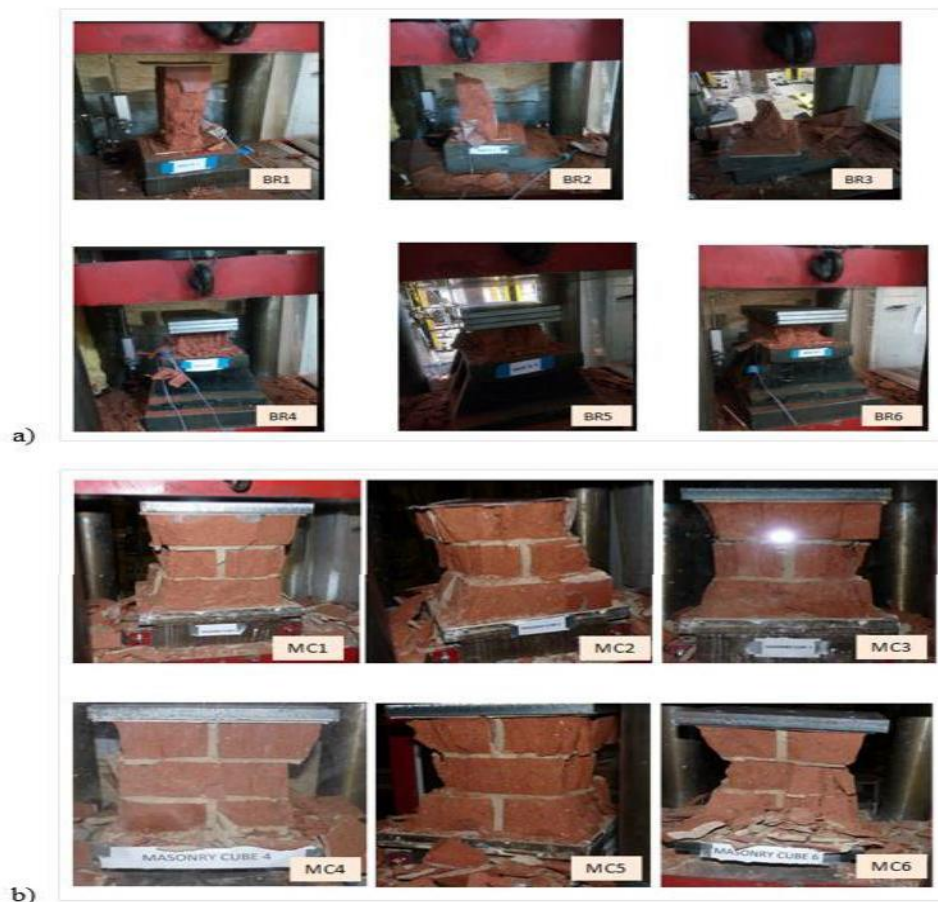

Figure 5: Failure modes of (a) brick units (b) masonry cube

4   NUMERICAL ANALYSIS

Finite Element (FE) modelling and analysis of masonry structures posed some of the greatest challenges to structural engineers. The main difficulty has been attributed to the presence of mortar joints which act as the major planes of weakness, discontinuity and nonlinearity. In spite of all these challenges, three modelling techniques have evolved. The choice of the method to adopt depends on the level of material information available, level of accuracy and simplicity desired [9]. In this study, the detailed micro-modelling has been adopted. In this strategy, units and mortar joints are represented by 3D continuum elements while the unit–mortar interface is represented by discontinuum elements. This technique produces the most accurate results, but it's computationally intensive due to the detailed level of refinement [9].

4.1   Finite element model description

Masonry cube model was created using a three-dimensional solid (or continuum) elements in ABAQUS. In particular, hexahedral element C3D8R which have an improve convergence and accuracy was selected to generate the mesh that represents the brick and mortar. The size of the units is 215 x 102.5 x 65mm and the thickness of mortar joint is 10mm. The bricks unit and mortar joint (bed and perpend) were defined using their respective own mechanical properties (Table 3-6). The nonlinearity of masonry and the interaction of brick/mortar interface have been considered and modelled using the constitutive models (concrete damage plasticity (CDP)) and kept elastic at present stage.

4.2   Constitutive model
4.2.1   Concrete damage plasticity (CDP)

The Concrete Damage Plasticity model available in ABAQUS material library was used to simulate the non-linear behaviour of masonry unit and the mortar in the numerical simulation of masonry cube. The CDP models assume a non-associated potential plastic flow which is an adoption of Drucker-Prager hyperbolic function for flow potential [23]. The failure modes recognise by CDP models are crack in tension or crushing in compression and the responses can be described as shown in figure 6 for masonry unit to figure 8 for mortar. The equivalent uniaxial stress-strain relationship and corresponding damage parameter for the models used in this study were based on primary models found in [23, 27].

4.2.2   CDP for masonry units

The CDP data for both compressive and tensile behaviour of masonry units were computed and figure 7 shows how the schematic stress-strain relationship used in this study compared to what is described in [23]. The curve has three different regions, and the formulations for each region are shown from equations 2 to 12 derived [24-26]. The compressive strength and modulus of elasticity of brick units obtained experimentally were used in these equations.

Referring to figure 6(a) for tensile behaviour of masonry unit
   i) The first region: elastic region (A to B)
$$f_{tb} = E_{ib} * \varepsilon_{cr} \tag{2}$$
$$f_{tb} = 0.3 * (f_b)^{2/3} \tag{3}$$
   ii) The second region: inelastic region (B to C)
$$\sigma_t = (f_{tb} * x)/(\alpha_t (x-1)^{1.7} + x) \tag{4}$$
$$x = \varepsilon_t / \varepsilon_{cr} \tag{5}$$
$$\alpha_t = 0.312 f_{tb} \tag{6}$$

Referring to figure 6(b) for compressive behaviour of masonry unit
  i) The First Region: Elastic Region (A to B)

$$\sigma_c = E_{ib} * \varepsilon_c \qquad (7)$$

 ii) The Second Region: Inelastic Region (B to C i.e. $x \leq 1$)

$$\sigma_c = (\propto_a x + (3 - 2 \propto_a)x^2 + (\propto_a - 2)x^3) * f_b \qquad (8)$$

iii) The third region: inelastic region (C to D i.e. $x \geq 1$)

$$\sigma_c = f_b/(\propto_d x(x-1)^2) \qquad (9)$$

$$x = \varepsilon_c/\varepsilon_{c1} \qquad (10)$$

$$\propto_a = E_{ib}/E_b \qquad (11)$$
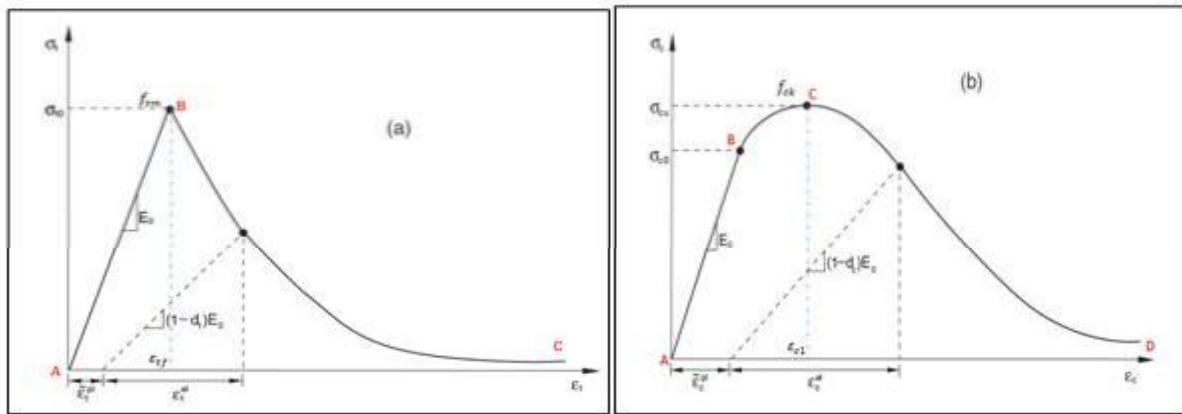
$$1.5 \leq \propto_d \leq 3 \qquad (12)$$

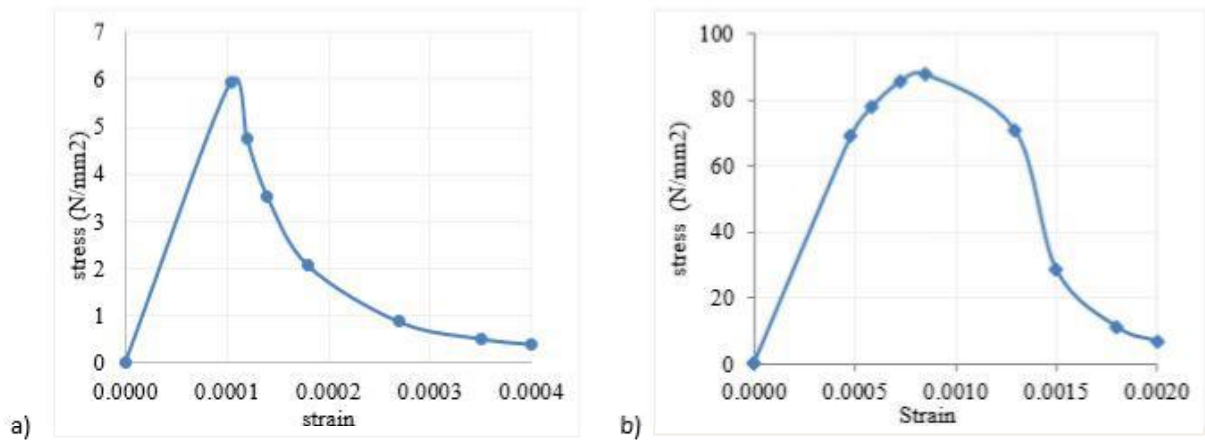Figure 6: Response of concrete to uniaxial loading (a) tensile (b) compressive [23]

Figure 7: Response of brick unit to uniaxial loading (a) tensile (b) compressive

4.2.3   CDP for mortar

In order to plot the strain-strain relationship to simulate the behaviour of the mortar, the procedures highlighted in [27] was used. The only availabe direct measurement from the tests is the average compressive strength (fcm) of the mortar. Other quantities such as longitudinal modulus of elasticity (Ecm) of the mortar, compressive stress and shortening strain were calculated using the eqn 13-20 as found in [27,28].

Referring to figure 8(a) for tensile behaviour of mortar

The tensile strength of the mortar was not determined experimentally but equation 13 stated in [27] was used to calculate this. To simulate the tensile behaviour of mortar, equation 14-15 was used. As described in [23], tensile stress of concrete can be linearly reduced to zero, starting from the moment of reaching the tensile strength, this was done and the resulting stress-strain curve was compared to the description in [23,27] as shown in figure 9.

$$f_{ctm} = 0.3 * (f_{cm})^{2/3} \qquad (13)$$
$$\sigma_t = E_{cm} * \varepsilon_t \quad if \ \varepsilon_t \leq \varepsilon_{cr} \qquad (14)$$
$$\sigma_t = f_{cm} * (\varepsilon_{cr}/\varepsilon_t)^{0.4} \ if \ \varepsilon_t > \varepsilon_{cr} \qquad (15)$$

Referring to figure 8(b) for compressive behaviour of mortar

The compressive stress were calculated as follows and the plot of data obtained was compared to the standard chart given in EC2

$$\sigma_c = f_{cm}(k\eta - \eta^2)/(1 + (k-2)\eta) \qquad (16)$$
$$k = 1.05 E_{cm} * (\varepsilon_{c1}/f_{cm}) \qquad (17)$$
$$\eta = \varepsilon_c/\varepsilon_{c1} \qquad (18)$$
$$E_{cm} = 22 * (f_{cm}/10)^{0.3} \ \text{GPa} \qquad (19)$$
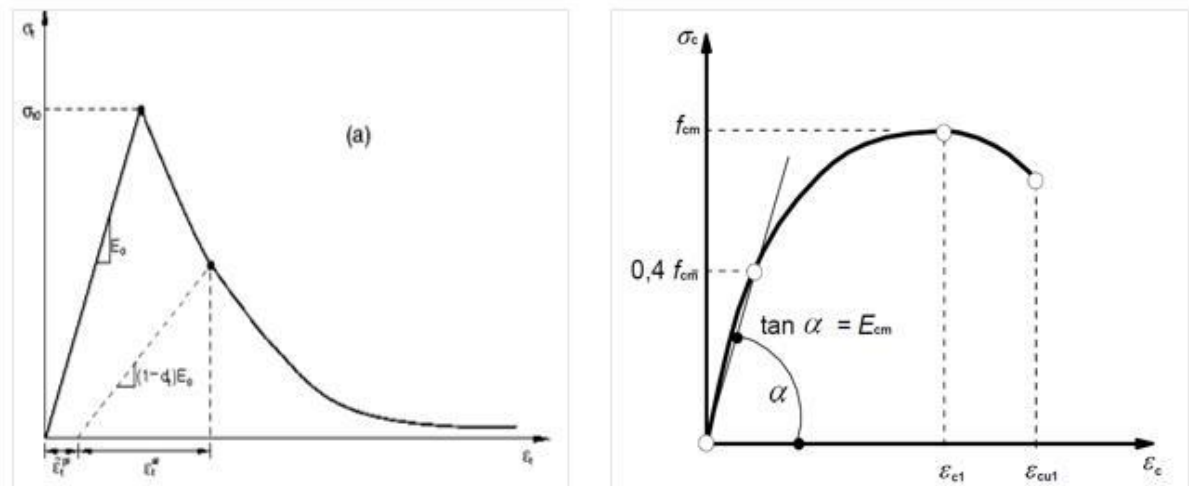$$\varepsilon_{c1} = 0.7 * (f_{cm})^{0.31} \qquad (20)$$

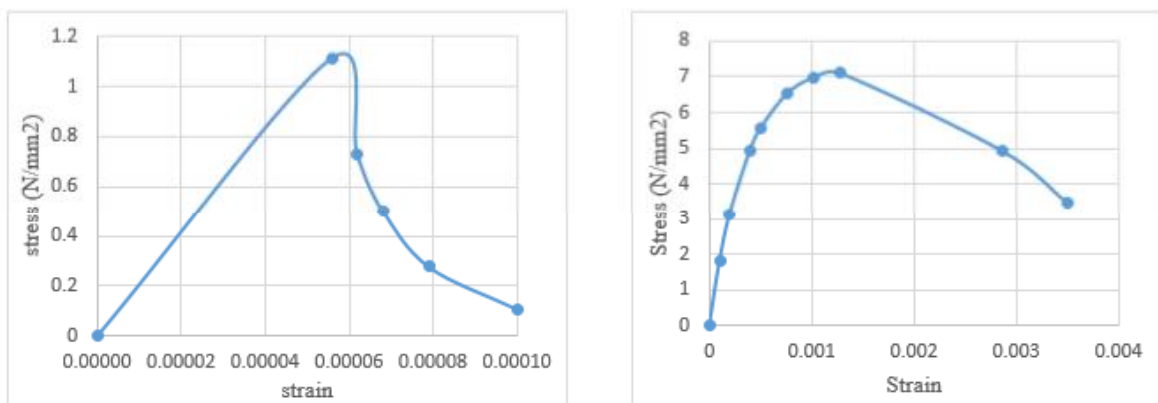Figure 8: Response of concrete to uniaxial loading (a) tensile [23] (b) compressive [27]

Figure 9: Response of mortar to uniaxial loading (a) tensile (b) compressive

4.3   Model input parameter

Elasticity parameters	Symbol	Value	
		Masonry unit	**Mortar**
Mass density (tonne/mm^3)	γ	2200e-12	-
Young modulus (N/mm^2)	E	32470	19850
Poisson ratio	μ	0.26	0.2

Plasticity parameters			Ref/comments
Dilation angle	Ψ	30	
Eccentricity parameter	e	0.1	0-0.1 from theory of Drucker-Prager
Bi and unidirectional compressive strength ratio	f_{bo}/f_{co}	1.16	Given as default value in ABAQUS
Stress ratio in tensile meridian	k	0.67	for regularisation of constitutive equation in ABAQUS
Viscosity parameter	υ	0.001	for convergence in ABAQUS

Table 3: Mechanical properties of masonry unit and mortar

Compressive behavior		Tensile behavior	
Yield stress (N/mm^2)	Inelastic strain	Yield stress(N/mm^2)	Cracking strain
26.37	0.00000	5.93	0.00000
69.09	0.00002	4.76	0.00002
77.65	0.00012	3.54	0.00004
85.46	0.00026	2.07	0.00008
87.91	0.00039	0.87	0.00017
70.92	0.00083	0.51	0.00025
28.40	0.00104	0.39	0.00030
11.08	0.00134		
6.80	0.00154		

Table 4: Concrete damage plasticity of masonry unit

Compressive behavior		Tensile behavior	
Yield stress (N/mm^2)	Inelastic strain	Yield stress(N/mm^2)	Cracking strain
1.79	0.00000	1.11	0.000000
3.13	0.00010	0.73	0.000006
4.93	0.00030	0.50	0.000012
5.58	0.00041	0.28	0.000023
6.53	0.00067	0.11	0.000044
6.97	0.00092		
7.10	0.00119		
4.92	0.00277		
3.48	0.00340		

Table 5: Concrete damage plasticity of mortar

4.4 Model output

Figure 10 shows the general assemblage of the masonry cube, FE mesh and the boundary condition. The nodes at the bottom of the cube were restrained in all the three direction (x, y, z) to replicate the friction in test condition of the specimen.
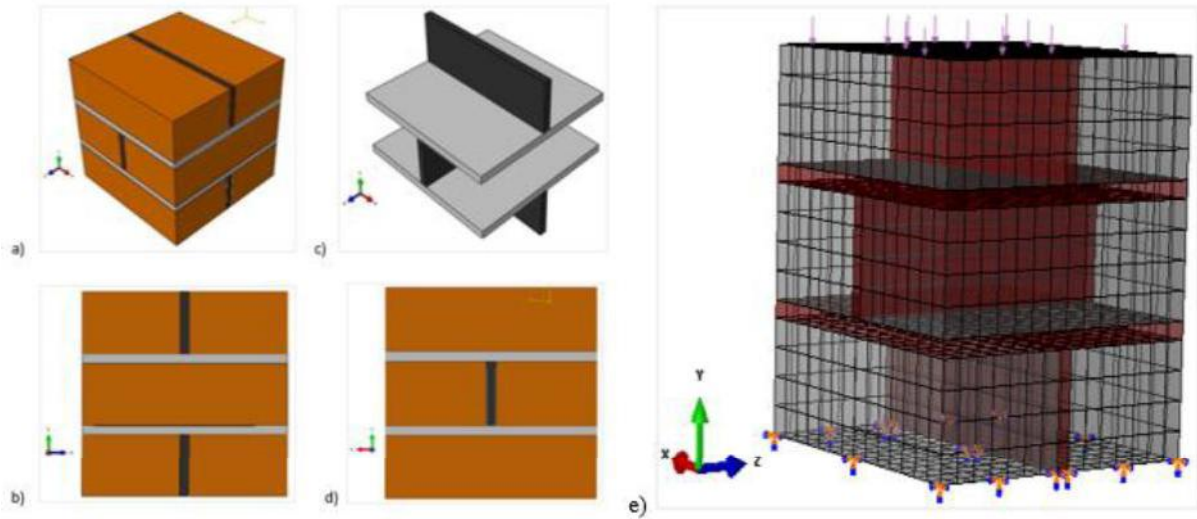

Figure 10: a) Micro modelling of masonry cube; (b) mortar joint (c) front elevation (d) side elevation (e) FE mesh, boundary condition and surface interaction
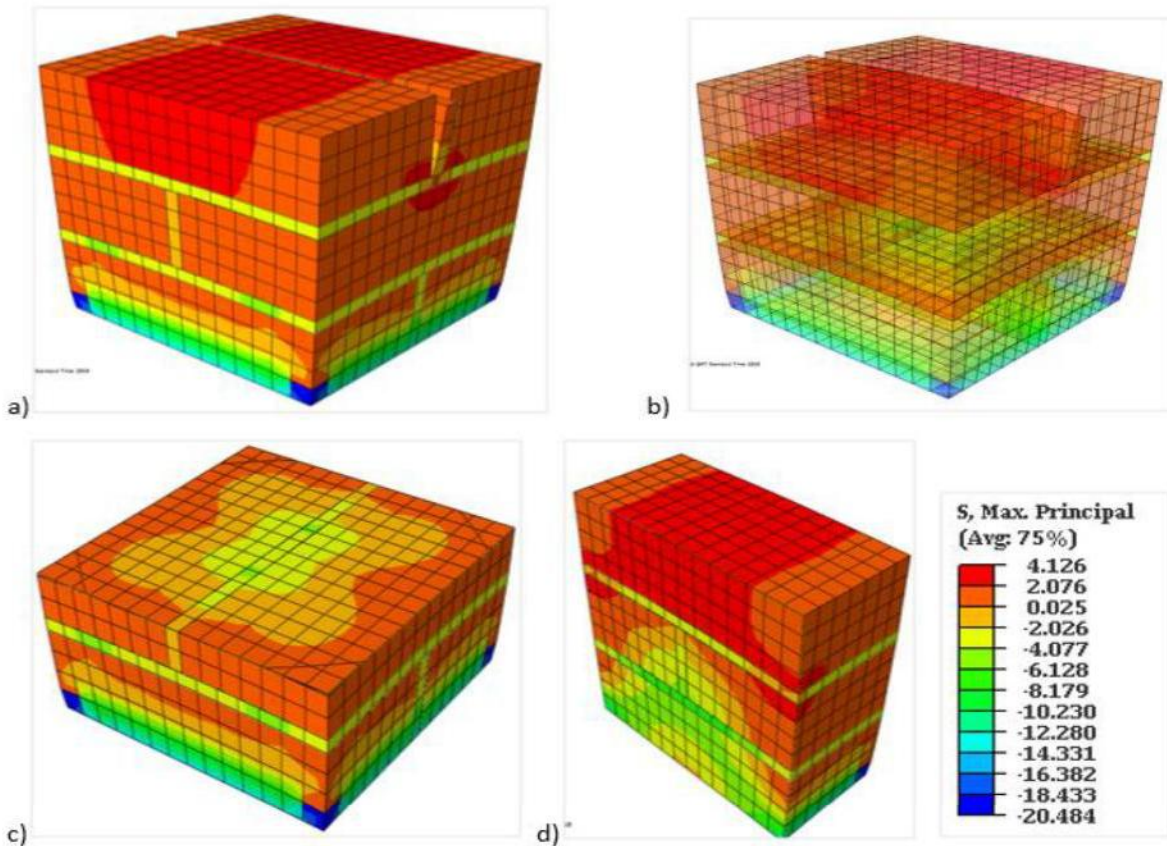

Figure 10: Principal stress (a) whole model (b) wireframe view to show what happen to mortar joint (c) view cut along x-plane (d) view cut across y-plane

Figure 11 shows the maximum principal stress in the masonry prisms. The maximum stress obtained from the numerical model is $20.5 N/mm^2$. This values compared to $(22.6 N/mm^2)$ which is the compressive strength of masonry obtained using the properties of masonry unit and mortar obtained experimentally by applying equation 1 stated earlier has a difference of 9%. This value compared fairly well considering that fact that the strength of the unit is high.

However, as deduced from the model output, the failure mode is similar to what was observed experimentally with the maximum compressive stress occurring at the bottom edges of the cube. The stress diagram also showing that there is a tensile stress in the mortar joint (Fig. 10b). This ultimately leads to the tensile splitting of the brick units and that explains what happen in the test results as can be seen from figure 5.

5   CONCLUSIONS

This paper presents experimental tests to characterized fire clay brick units and mortar that will be used for study of a proposed retrofit technique. Apart from testing each component individually, an unconventional test has been carried out to study the behavior of a masonry cube under compression loading. Based on the results of the mechanical properties of brick units and mortar, a detailed micro model of the masonry cube was developed and analyzed. The following conclusions were drawn;

- The proposed masonry units and mortar mix ratio will be suitable for the proposed experimental study because the combination of the two is similar to what is expected in old masonry units (strong unit-weak mortar joint). Hence, the material source will remain unchanged throughout the test.

- The use of detail micro modelling of masonry cube was able to predict the behavior and failure of masonry cube. The result gives a different of 9% between numerical values and value obtained using code. This shows that the model is able to predict the strength of the masonry, on the safe side.

- Although, the developed model has been proved to have prospect of predicting the behavior of masonry, more work is still required to capture the crack patterns of the bricks within the model.

REFERENCES

[1] A. Menon, G. Magenes, *Out-of-plane seismic response of unreinforced masonry: definition of seismic input.* Research report, European School for Advanced Studies in Reduction of Seismic Risk, IUSS Press, Pavia, (Italy), 2008.

[2] L. Ramos, P. Lourenço, *Modeling and vulnerability of historical city centers in seismic areas: a case study in Lisbon.* Engineering Structures, 26(9), pp.1295-1310, 2004.

[3] F. Seible, M. Priestley, G. Hegemier, D. Innamorato, *seismic retrofit of RC columns with continuous carbon fiber jackets.* Composites for Construction, 1(2), pp.52-62, 1997.

[4] P. Lourenço, N. Mendes, A. Costa, A. Campos-Costa, *Methods and challenges on the out-of-plane assessment of existing masonry buildings.* International Journal of Architectural Heritage, 11(1), pp.1-1, 2017.

[5] A. A. Costa, A. Arêde, A. Costa, C. Oliveira, *Out-of-plane behaviour of existing stone masonry buildings: experimental evaluation.* Earthquake Engineering, 10(1), pp.93-111, 2011.

[6] S. Hamoush, M. McGinley, P. Mlakar, D. Scott, K. Murray, *Out-of-plane strengthening of masonry walls with reinforced composite.* Composites for Construction, 5(3), pp.139-145, 2001.

[7]   A. Zeiny, J. Larralde, *Seismic evaluation of the performance of retrofitted and repaired brick walls by means of expansive epoxy injection*. [Online]. Available at: http://zeiny.net/FundedProjects/FoamReport/FoamReport.htm.[Accessed 3 Oct. 2017].

[8]   I. Sustersic, B. Dujic, *Seismic strengthening of existing concrete and masonry buildings with crosslam timber panels*. Materials and Joints in Timber Structures, pp.713, 2014.

[9]   P.B. Lourenço, *Computational strategies for masonry structures*. PhD Thesis, Delft University of Technology, Delft University Press, Delft (NL), 1996.

[10] ASTM E518-15, *Standard test methods for flexural bond strength of masonry*. West Conshohocken, PA: ASTM International, 2015.

[11] ASTM E72–15, *Standard test methods of conducting strength tests of panels for building construction*. West Conshohocken, PA: ASTM International, 2015.

[12] BS EN 772-13:2000, *Methods of test for masonry units: determination of net and gross dry density of masonry units (except for natural stone)*. London: British Standard Institution, 2000.

[13] BS EN 772-21:2011, *Methods of test for masonry units: determination of water absorption of clay and calcium silicate masonry units by cold water absorption*. London: British Standard Institution, 2011.

[14] BS EN 772-1:2011, *Methods of test for masonry units: determination of compressive strength*. London: British Standards Institution, 2011.

[15] D. Oliveira, R. Silva, E. Garbin, P. Lourenço, *Strengthening of three-leaf stone masonry walls: an experimental research*. Materials and Structures, 45(8), pp.1259-1276, 2012.

[16] G. Vasconcelos, P. Lourenço, *Experimental characterization of stone masonry in shear and compression*. Construction and Building Materials, 23(11), pp.3337-3345, 2009.

[17] BS 4551:2005, *Methods of test for mortar and screed: chemical analysis and physical testing*. London: British Standard Institution, 2005.

[18] BS EN 1015-3:1999, *Methods of test for mortar for masonry: determination of consistence of fresh mortar (by flow table)*. London: British Standard Institution, 1999.

[19] S. Arash, *Mechanical properties of masonry samples for theoretical modelling*. Florianópolis – Brazil: 15th International Brick and Block Masonry Conference, 2012

[20] V. Haach, G. Vasconcelos, P. Lourenço, G. Mohamad, Composition study of a mortar appropriate for masonry cavities and joints. USA: North American Masonry conference, pp.530-541, 2007.

[21] BS EN 1052-1:1999, *Methods of test for masonry-part1: determination of compressive strength*. London: British Standard Institution, 1999.

[22] BS EN 1996-1-1:2005, Design of masonry structures - part 1-1: general rules for reinforced and unreinforced masonry structures. London: British Standards Institution, 2005.

[23] Dassault Systemes, *Abaqus/CAE*. USA: Dassault Systemes Simulia Corp, 2014.

[24] B. Sinha, K. Gerstle, L. Tulin, stress-strain relations for concrete under cyclic loading. ACI Journal Proceedings, 61(2), pp.195-211, 1964.

[25] Z. Guo, *Principles of reinforced concrete*. 1st ed. Oxford, p.589, 2014.

[26] C. Santos, R. Alvarenga, J. Ribeiro, L. Castro, R. Silva, A. Santos, Nalon, *Numerical and experimental evaluation of masonry prisms by finite element method*. IBRACON Structures and material journal, 10(2), pp.477-508, 2017.

[27] BS EN 1992-1-2:2004, *Design of concrete structures: general rules, structural fire design*. London: British Standard Institution, 2004.

[28] T. Wang, T. Hsu, *Nonlinear finite element analysis of concrete structures using new constitutive models*. Computers & Structures, 79(32), pp.2781-2791, 2001.